Isothermal Titration Calorimetric Study of RNase-A Kinetics (cCMP → 3′-CMP) Involving End-Product Inhibition

Shawn D. Spencer[1] and Robert B. Raffa[1,2,3]

Received November 20, 2003; accepted May 17, 2004

Purpose. Isothermal titration calorimetry (ITC) and progress curve analysis was used to measure the enzyme kinetic parameters (K_M and k_{cat}) of the hydrolysis of cCMP by RNase-A, a reaction that includes end-product competitive inhibition by 3′-CMP.

Methods. The heat generated from injection of 9–15 μl cCMP (20 mM) into bovine pancreatic RNase-A (600 nM) in 50 mM Na^+ acetate buffer (pH 5.5; 37°C) was monitored for 1500–2000 s. Thermal power (dQ/dt), equal to (1) $/\Delta H_{app} \times d(\text{cCMP})/dt$ was recorded every 1 s. The end-product inhibition constant (K_p) and enthalpy of the inhibitor binding interaction was obtained from the saturation data of 60 sequential injections of 3′-CMP (1.2 mM) into 0.05 mM RNase-A. The data of the plot of $-d[\text{cCMP}]/dt$ against [cCMP] were fitted to kinetic equations incorporating K_p to yield K_M and k_{cat}.

Results. ΔH_{app} for each run was obtained by integration of the progress curve. The plot of $-d[\text{cCMP}]/dt$ against [cCMP] yielded the kinetic parameters K_M = 105.3 μM, 121.6 μM, and 131.3 μM; k_{cat} = 1.63 s^{-1}, 1.56 s^{-1}, and 1.71 s^{-1}. The end-product bound with 1:1 stoichiometry and K_p = 53.2 μM.

Conclusions. The combination of progress curve analysis and ITC allowed rapid and facile measurement of the kinetic parameters for catalytic conversion of cCMP to 3′-CMP by RNase-A, a reaction complicated by end-product inhibition.

KEY WORDS: calorimetry; end-product inhibition; enzyme kinetics; RNase.

INTRODUCTION

RNases (ribonucleases) constitute a family of cellular exo- and endonuclease [EC 3.1.27.5] enzymes that are present in vertebrates, bacteria (1,2,3), mold (4), and plants (5,6). They perform important functions in the processing of RNA, which has been estimated to comprise about 20% of a cell's dry mass (1). However, RNases can be overtly toxic (7) or can exacerbate pathologic conditions. For example: angiogenin, an RNase found in plasma, induces angioneogenesis in tumors (8); RNase-2 (RNase U) is neurotoxic and may produce some of the symptoms associated with overproduction of eosinophils (9); and bovine seminal RNase is immunosuppressive, embryotoxic, and aspermatogenic (10). Hence, either activators or inhibitors of RNases could have therapeutic potential as novel pharmaceutical agents.

RNases display a preference for pyrimidine bases (cytosine and uracil) of RNA. The catalytic mechanism of RNA cleavage by RNases is thought to occur in two steps (11). In the first step, a 2′,3′-cyclic phosphodiester is formed by a "transphosphorylation" reaction from the 5′ carbon to the 2′ carbon of the next nucleotide in the RNA chain. Specific amino acid residues of the RNase form the catalytic reaction domain, the details of which have been determined by several strategies, including chemical modification and site-directed mutagenesis studies (e.g., 12–15). In the second step, the subject of the present report, the product of the first step (2′,3′-cyclic phosphodiester) is hydrolyzed to a 3′ nucleotide (3′-CMP) (16,17) (Fig. 1). Both of these reactions are catalyzed by RNase. A complication in obtaining kinetic parameters for this reaction arises because 3′-CMP is an inhibitor of RNase-A and, thus, results in end-product inhibition of the overall reaction.

Isothermal titration (micro)calorimetry (ITC) is a highly accurate and automated technique that directly measures the apparent enthalpy change (ΔH_{app}) associated with reactions in solution and it is used to obtain thermodynamic parameters for ligand-macromolecule interations (18). In the standard ITC apparatus, the reaction proceeds in a sample cell of relatively small volume (usually 1–2 ml). One component of the reaction is already in the reaction cell (e.g., enzyme), the other component (e.g., substrate or inhibitor) is added by an automated injection system in measured amounts for measured times. A stirrer ensures that the reaction is continuously and well mixed. The reaction cell is composed of material of good thermal conductivity such that energy changes occurring within the reaction cell are transmitted as temperature changes. In modern ITC equipment the change is measured as the differential current (power) that is required to maintain the reaction cell at the same pre-set temperature of a reference cell. Thus, the measurements are highly precise and reproducible. Following each injection, the power is recorded as a function of time. If the reaction is exothermic, less thermal power (J s^{-1}) is required relative to the reference cell; if the reaction is endothermic, more power is required (the total system is closely maintained at a preset temperature). Details about ITC are available in several excellent reviews (19–21).

Todd and Gomez (22) have described techniques for determining enzyme kinetic constants using ITC based on the proportionality between the rate of a reaction and the thermal power generated, but did not examine RNase. Cai *et al.* (23) used ITC to examine RNase-A, but used the initial rate approximation. Koerber and Frank (24) examined hydrolysis of 3′-CMP by RNase-A using a new method based on numerical differentiation of the complete reaction (progress) curve in which data are fitted to the rate equation itself (25)—which they showed had advantages over initial velocity or integrated Michaelis-Menten equation methods—but measured enzyme activity spectrophotometrically. The present study is the first, to our knowledge, to combine the advantages of ITC and differential analysis of the progress curve to the enzymatic conversion of cCMP to 3′-CMP by RNase-A, which involves end-product inhibition by 3′-CMP.

MATERIALS AND METHODS

Materials

Bovine pancreatic RNase (RNase-A, type XII-A, EC 3.1.27.5), cCMP (2′,3′- CMP; 2′,3′-cyclic cytidine monophosphate), and 3′-CMP were purchased from Sigma-Aldrich (St. Louis, MO). Buffer chemicals, analytical grade, were pur-

[1] Department of Pharmaceutical Sciences, School of Pharmacy, Temple University, Philadelphia, Pennsylvania 19140, USA.
[2] Department of Pharmacology, School of Medicine, Temple University, Philadelphia, Pennsylvania 19140, USA.
[3] To whom correspondence should be addressed. (e-mail: robert.raffa@temple.edu)

0724-8741/04/0900-1642/0

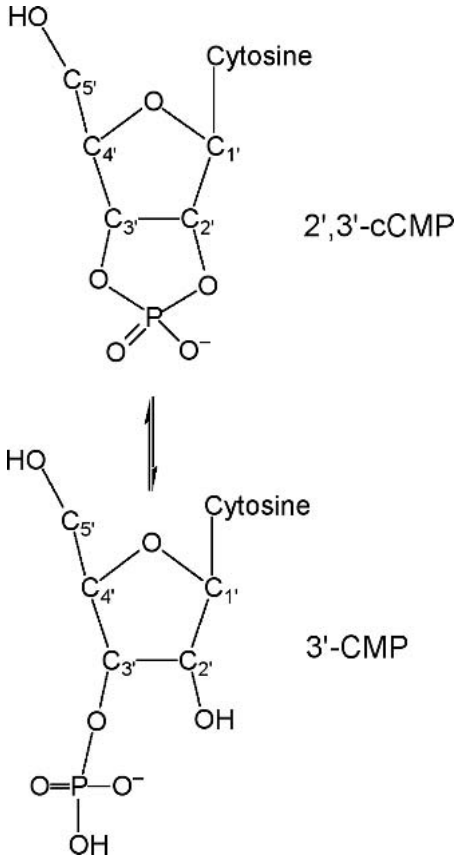

Fig. 1. Reaction scheme for the two-step catalytic action of RNase-A. RNA is the substrate for the first transphosphorylation reaction, and 2′,3′-cyclic CMP (cCMP) is the product which, in turn, is the substrate for the second hydrolysis reaction that produced 3′-CMP.

chased from VWR Scientific (Bridgewater, NJ). The microcalorimeter (model VP-ITC) was purchased from MicroCal LLC (Northampton, MA).

Kinetic Parameters

The reaction mechanism for the interaction between RNase-A (E) and cCMP (S) to form 3′-CMP (P) is represented by:

$$\mathrm{E} + \mathrm{S} \underset{k_{-1}}{\overset{k_1}{\Leftrightarrow}} ES \overset{k_{\mathrm{cat}}}{\rightarrow} \mathrm{E} + \mathrm{P},$$

where k_{cat} is the catalytic rate (substrate turnover rate) constant and $(k_{-1} + k_{\mathrm{cat}})/k_1$ is the Michaelis-Menten constant (K_{M}). In a calorimeter, the rate of a reaction is related to the measured heat by the following equation (22):

$$Rate = \frac{d[P]}{dt} = -\frac{d[S]}{dt} = \frac{1}{V \cdot H_{\mathrm{app}}} \cdot \frac{dQ}{dt}, \tag{1}$$

where $[S]$ and $[P]$ are the molar concentrations of the substrate (cCMP) and product (3′-CMP), respectively, V is the volume of the reaction cell, ΔH_{app} is the (apparent) molar enthalpy for the reaction, and dQ/dt is the thermal power, which is the rate of change of heat (Q) with respect to time (t). Equation 1 is obtained from the rate equality:

$$-\frac{d[S]}{dt} = \frac{d[P]}{dt}, \tag{2}$$

and the amount of heat associated with converting n moles of substrate into product:

$$Q = n \cdot \Delta H_{\mathrm{app}} = [P]_{\mathrm{total}} \cdot V \cdot \Delta H_{\mathrm{app}}. \tag{3}$$

The magnitude of the experimentally-measured apparent molar enthalpy change (ΔH_{app}) approaches the magnitude of the intrinsic enthalpy change (ΔH_{int}) when the reaction is conducted in buffers that have a small heat of ionization (ΔH_{ion}) such as acetate (26), since $\Delta H_{\mathrm{app}} = \Delta H_{\mathrm{int}} + \eta \Delta H_{\mathrm{ion}}$ where η is the number or protons released from the buffer. A plot of $-d[S]/dt$ against $[S]$ (i.e., $-d$[cCMP]$/dt$ against [cCMP]) yields the kinetic parameters from the steady-state rate equation for the general case of noncooperative, single-substrate, single-product enzymatic catalysis (24):

$$\frac{d[P]}{dt} = \frac{\dfrac{V_{\mathrm{M}}[S]}{\left(1 - K_{\mathrm{M}} \Big/ K_{\mathrm{p}}\right)}}{\dfrac{[S_0] + K_{\mathrm{p}}}{\left(K_{\mathrm{M}} \Big/ K_{\mathrm{P}} - 1\right)} + [S]}, \tag{4}$$

where the end-product affinity (K_{p}) can either be estimated as a fitting parameter or, as done in the present experiments, can be obtained from a separate determination of the binding of end-product (3′-CMP) with enzyme (RNase-A).

Procedure

The ITC instrumentation (VP-ITC Microcal, LLC, Northampton, MA) has been described previously (27). In short, the data collection involves monitoring the electrical power supplied to the compensation heater attached to the reaction cell that is required to maintain isothermal conditions. Thus, the measured experimental quantity is the energy (heat) flow from the sample cell, which is directly proportional to the heat of the reaction. Following an injection of reactant into the reaction cell, the power supplied (or conserved) to compensate for the reaction heat is evident as a departure from baseline, attainment of a maximum excursion, and return to baseline once catalysis is complete. The trapezoidal rule yields the area under the curve between two data points that were collected every second, and integration yields the total AUC, which is Q for the reaction. The ratio AUC/n, where n is the number of moles of substrate injected, yields ΔH_{app}.

RNase-A and cCMP solutions were degassed under vacuum for 10 min. A 250 μL syringe was filled with cCMP (20 mM) dissolved in 50 mM Na^+-acetate buffer (pH 5.5). The 1.4 ml reaction vessel (maintained at 37°) was filled with RNase-A (600 nM, determined spectrophotometrically at 280 nm using $\varepsilon = 9800\ \mathrm{cm^{-1}\ m^{-1}}$) in 50 mM Na^+-acetate buffer (pH 5.5) and stirred at 270 rpm. The result of single injections of 9–15 μl was monitored for 1500–2000 s (to allow time for substrate depletion) and the thermal power (dQ/dt) in watts was recorded every 1 s. The data were fit to kinetic equations using WINNONLIN (Scientific Consulting, Inc., Mountain View, CA). The affinity constant of the 3′-CMP end-product (K_{p}) was obtained using 60 injections of 3′-CMP (1.2 mM)

into 0.05 mM RNase-A using methods described for the binding of 2′-CMP in prior publications (28,29).

RESULTS

End-Product Binding

The selected conditions produced heats for the interaction 3′-CMP + RNase-A ⇔ 3′-CMP–RNase-A that yielded consistent isotherms such as that shown in Fig. 2 (top). A stable baseline was maintained over the course of the 60 injections of 3′-CMP (1.2 mM) into RNase-A (0.05 mM). Each downward deflection in the figure corresponds to heat generation of the exothermic reaction. The progressively smaller heat output of each injection corresponds to saturation of RNase-A binding sites by 3′-CMP. The heat of dilution was determined from 10 additional injections into saturated enzyme (same result as into buffer), and was subtracted from the reaction heat. The total time for each of the 3 replicate runs was 6 h (60 injections × 360 s per interval). The maximal output was generally 1.5–2 μcal s^{-1} (6–8 μJ s^{-1}). The data were processed and deconvoluted using ORIGIN software (v 5.0, MicroCal Software, Northampton, MA). The transposed data were normalized per mole of 3′-CMP injected by integration and were plotted as the integrated heats (Fig. 2, bottom). A curve was obtained by computer-generated fit to a single-site binding model using nonlinear regression. From the fitting parameters a stoichiometry of 1:1 was obtained with $K_p = 53.2 \pm 1.5$ μM and $\Delta H_{app} = -17.7 \pm 1.1$ kcal mol^{-1} (–74.0 ± 4.6 kJ mol^{-1}).

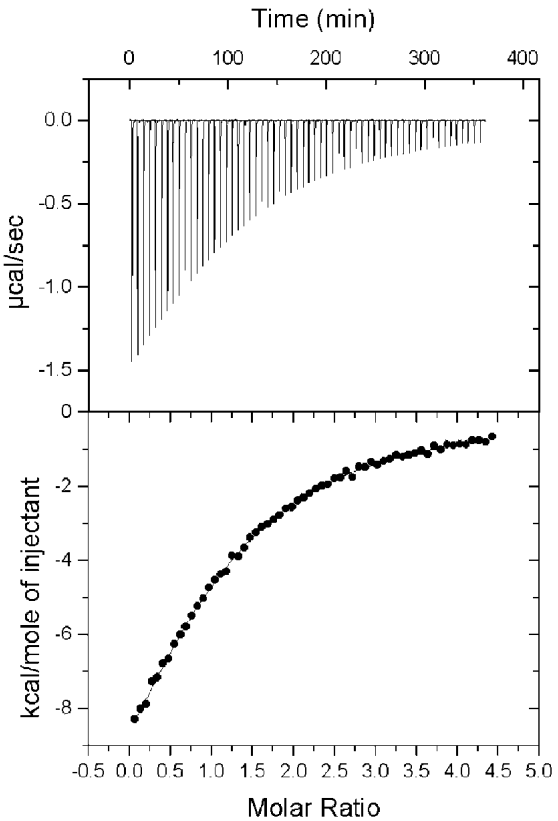

Fig. 2. Representative isotherm for the binding of 3′-CMP to RNase-A. Top: raw data output of power (heat released) for each of 60 consecutive injections of 3′-CMP (1.2 mM) into RNase-A (0.05 mM) at 37°C (pH 5.5). Bottom: heat exchange at each injection obtained by integration of each injection "spike" in the top panel, normalized to kcal mol^{-1} of 3′-CMP. The line is the computer-generated best-fit to a single-site binding model.

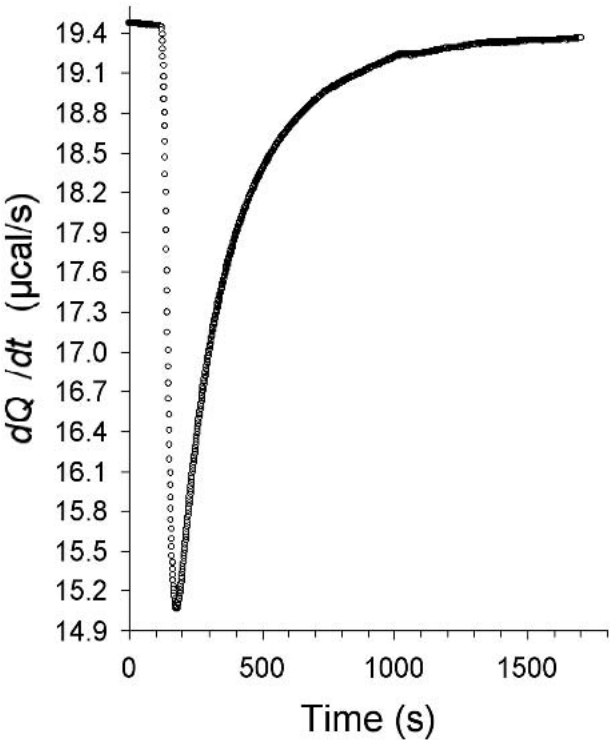

Fig. 3. Representative isotherm monitored for 1500 s following a single injection of cCMP (20 mM) into 600 nM of RNase-A at 37°C (pH 5.5).

Kinetics

Single injection of cCMP (20 mM) into RNase-A (600 nM) produced heat from the catalytic conversion cCMP → 3′-CMP that was detected as a downward deflection in the isotherm, indicative of an exothermic interaction (Fig. 3). Maximum heat output was obtained between 60 and 80 s after injection. The system returned to baseline, indicative of complete conversion of substrate (cCMP) to product (3′-CMP), between 1500 and 2000 s. Conversion followed apparent first-order reaction kinetics, as shown by a plot of the decline of cCMP and increase of 3′-CMP with time (Fig. 4).

A series of 35 injections each yielded ΔH_{app} according to the integrated form of Eq. 1,

$$\Delta H_{app} = \frac{1}{[\text{cCMP}]_0 \cdot V} \cdot \int_{t=0}^{t} dQ, \qquad (5)$$

which gave substrate concentration as a function of time according to:

$$[\text{cCMP}] = [\text{cCMP}]_0 - [3' - \text{CMP} = [\text{cCMP}]_0 - \frac{\int_{t=0}^{t} Q}{V \cdot \Delta H_{app}}. \qquad (6)$$

The graph of $d[3'\text{-CMP}]/dt$ is shown in Fig. 5. The data were fitted to Eq. 4 using WINNONLIN (Scientific Consulting, Inc., Mountain View, CA) software, yielding K_M and k_{cat} as fitted parameters (Table I).

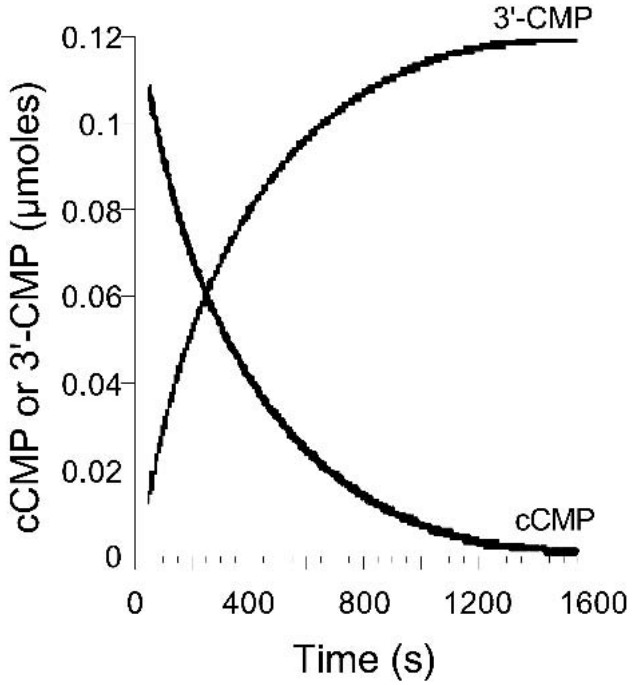

Fig. 4. Same data as in Fig. 3 plotted as the time-dependent depletion of substrate (cCMP) and generation of product (3′-CMP).

DISCUSSION

Members of the RNase superfamily have both intracellular ('non-secretory') and extracellular ("secretory") (30,31) roles that contribute to their beneficial and desirable functions. However, under certain circumstances, RNases can be cytotoxic. An example is stimulation of blood vessel proliferation (angioneogenesis) in tumors by the blood-borne RNase angiogenin. Another is RNase-2, which is implicated in conditions where eosinophils appear in excess numbers, such as asthma and other inflammatory disorders in which tissue damage occurs as part of an allergic response (e.g., 32–34). For either its beneficial or deleterious roles, RNases

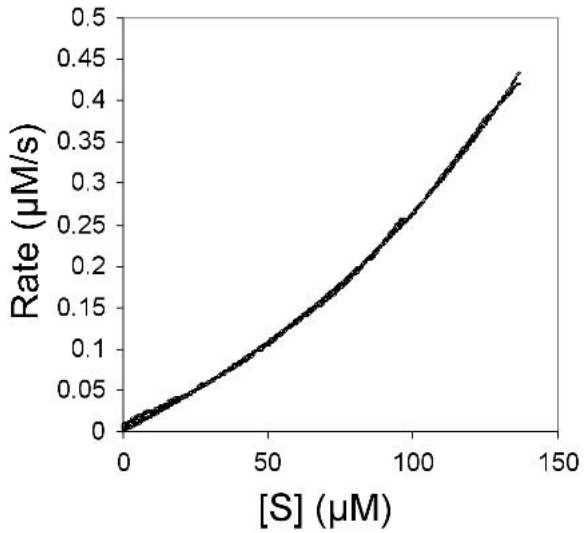

Fig. 5. Cumulative rate data for the catalytic hydrolysis of cCMP to 3′-CMP by RNase-A. The line is the best-fit computer-generated nonlinear regression to Eq. 4.

Table I. Kinetic Constants (K_M and k_{cat}) for Enzymatic Conversion of cCMP to 3′-CMP by RNase A Determined Using ITC and Progress Curve Analysis

	140 µM cCMP	185 µM cCMP	230 µM cCMP
K_M	105.3 ± 12.1	121.6 ± 14.5	131.3 ± 9.3
k_{cat}	1.63 ± 0.25	1.56 ± 0.02	1.71 ± 0.07

Values are the means ± SD of three independent measurements (37°C, pH 5.5).

are important enzymes to study—and potential modulators are being designed (35). RNase-A is the prototypic and most commonly studied representative of the RNase family.

Enzyme kinetics equations are usually formulated in terms of the dependence of reaction rate upon the concentration of substrate, whereas most studies measure the amount of substrate depletion or product generation. The usual way this is resolved is to analytically differentiate the data at zero-time and measure the initial rate of the reaction. Because instantaneous velocity is generally not possible to measure, it is necessary to define conditions where the progress curve is approximately straight for a measurable period of time. Since the reaction rate is maximum at the initiation of the reaction, the initial reaction rate is usually chosen. At less than about 1–5% reaction progress, and under appropriate experimental conditions, the initial-rate approximations yield adequate measurements for enzymatic biochemical reactions (36). However, for more complicated reactions, such as those that generate products that significantly inhibit enzyme activity (end-product inhibition), the practical requirements and interpretation become more restrictive. It is sometimes preferable that instead of initial rate analysis, the reaction "progress curve" can be differentiated or integrated and then fitted to the appropriate, usually Michaelis-Menten, model equation. In the *integral* method, continuous data (i.e., [*P*] vs. time) are fitted to an integrated rate equation; in the *differential* method, the experimental data, that is,, rate versus [*S*] ("progress curve") are fitted to a rate equation without transformation. Both continuous methods offer the advantage of utilizing the greater amount of the kinetic information contained in the entire progress curve, although such techniques can be computationally difficult. However, numerical differential methods for enzyme kinetic analysis, made practical with the introduction of computer-assisted data acquisition of large data-point collection, now allow accurate determination even for reactions that exhibit strong product inhibition (24). With the advent of modern power-compensated microcalorimeters with fast response-time, equipment is now able to take advantage of direct (not calculated) differential analysis. This circumvents the use of the integrated Michaelis-Menten equation and allows the advantages of full progress curve analysis. ITC already is used successfully to measure the thermodynamic parameters of biochemical reactions (e.g., see reviews 19, 20, 21), with application to drug-receptor interactions (18,37). The goal of the present study was to extend our ongoing study of RNase-A with ITC (28,29) to measure the kinetic constants for the RNase-catalyzed conversion of cCMP to 3′-CMP, a reaction with strong end-product inhibition.

The kinetic equations incorporating end-product inhibition include a term for the ΔH_{app} of the binding of end-

product to the enzyme as shown in equation [4] (viz., 3′-CMP to RNase-A in the present study). The enthalpy change term for this part of the overall reaction was obtained by independent determination by standard ITC methods, which we used previously for the study of the interaction of 2′-CMP with RNase-A (28,29). The advantage of ITC is the ability to easily and rapidly dissect out this portion of the overall reaction and the ready availability of the components of the RNase-A reaction. The stoichiometry of the interaction was found to be 1:1, the ΔH_{app} –17.7 ± 1.1 kcal mol^{-1} (–74.0 ± 4.6 kJ mol^{-1}), and the affinity constant K_p was 53.2 μM. The use of acetate buffer enhances the accuracy of ΔH_{app} determinations, because of its small ΔH_{ion} (26).

Substitution of the measured values for ΔH_{app} and K_p as fixed parameters into the kinetic equations allowed the determination of the kinetic parameters K_M and k_{cat} from the isotherms generated by injection of 3′-CMP into the reaction cell containing RNase-A. In our experiment, the Michaelis constant K_M = 105.3 μM, 121.6μM, and 131.3μM and the k_{cat} (turnover rate) = 1.63 s^{-1}, 1.56 s^{-1}, and 1.71 s^{-1}, depending on the initial substrate concentration. As expected, the turnover rate was essentially independent of initial substrate concentration. These values are in close agreement with the only comparative literature values (K_P = 72 μM, k_{cat} = 2.2 s^{-1}, and K_M = 820 μM) (39). The differences are probably attributable to the different technique (flow microcalorimetry) and slightly different buffer used in the prior study. The ease with which these values were determined highlights the extension of the use of ITC methodology to enzyme kinetics analysis (22,23,38). The advantages of ITC are well known, including ease, sensitivity, speed, direct determination of ΔH_{app}, ability to measure parameters of opaque solutions, and others (19–21).

CONCLUSIONS

ITC provided a rapid and facile means to measure the enzyme kinetic constants for the catalytic hydrolysis of cCMP to 3′-CMP by RNase-A, a reaction complicated by end-product inhibition. The procedure used differential analysis of the reaction progress curve, which avoids reliance on initial parameter estimation and uses all of the information in a reaction progress curve.

REFERENCES

1. A. W. Nicholson. Function, mechanism and regulation of bacterial ribonucleases. *FEMS Microbiol. Rev.* **23**:371–390 (1999).
2. R. W. Hartley. Barnase and barstar. In G. D. D'Alessio and J. F. Riordan (eds.), *Ribonucleases: Structures and Functions*, Academic Press, New York, 1997, pp. 51–100.
3. M. Irie, K. Nitta, and T. Nonaka. Biochemistry of frog ribonucleases. *Cell. Mol. Life Sci.* **54**:775–784 (1998).
4. I. G. Wool. Structure and mechanism of action of the cytotoxic ribonuclease -sarcin. In G. D. D'Alessio and J. F. Riordan (eds.), *Ribonucleases: Structures and Functions*, Academic Press, New York, 1997, pp. 131–162.
5. P. A. Bariola and P. J. Green. Plant ribonucleases. In G. D. D'Alessio and J. F. Riordan (eds.), *Ribonucleases: Structures and Functions*, Academic Press, New York, 1997, pp. 163–190.
6. S. K. Parry, Y.-H. Liu, A. E. Clarke, and E. Newbigin. S-RNases and other plant extracellular ribonucleases. In G. D. D'Alessio and J. F. Riordan (eds.), *Ribonucleases: Structures and Functions*, Academic Press, New York, 1997, pp. 191–211.
7. S. Sorrentino and M. Libonati. Structure-function relationships in human ribonucleases: main distinctive features of the major RNase types. *FEBS Lett.* **404**:1–5 (1997).
8. D. J. Strydom. The Angiogenins. *Cell. Mol. Life Sci.* **54**:811–824 (1998).
9. G. J. Gleich, D. A. Loegering, M. P. Bell, J. L. Checkel, S. J. Ackerman, and D. J. McKean. Biochemical and functional similarities between human eosinophil-derived neurotoxin and eosinophil cationic protein: homology with ribonuclease. *Proc. Natl. Acad. Sci. USA* **83**:3146–3150 (1986).
10. G. D'Alessio, A. Di Donato, L. Mazzarella, and R. Piccoli. Seminal ribonuclease: the importance of diversity. In G. D'Alessio and J. F. Riordan (eds.), *Ribonucleases: Structures and Functions*, Academic Press, New York, 1997, pp. 383–423.
11. C. M. Cuchillo, X. Pares, A. Guasch, T. Barman, F. Travers, and M. V. Nogues. The role of 2′,3′-cyclic phosphodiesters in the bovine pancreatic ribonuclease A catalysed cleavage of RNA: intermediates or products? *FEBS Lett.* **333**:207–210 (1993).
12. C. H. Hirs and J. H. Kycia. Identification of initial reaction sites in the dinitrophenylation of bovine pancreatic ribonuclease A. *Arch. Biochem. Biophys.* **111**:223–235 (1965).
13. M. S. Stern and M. S. Doscher. Aspartic acid-121 functions at the active site of bovine pancreatic ribonuclease. *FEBS Lett.* **171**:253–256 (1984).
14. K. Haydock, C. Lim, and A. T. Brunger. and M. Karplus M. Simulation analysis of structures on the reaction pathway of RNase A. *J. Am. Chem. Soc.* **112**:3826–3831 (1990).
15. G. L. Gilliland. Crystallographic studies of ribonuclease complexes. In G. D. D'Alessio and J. F. Riordan (eds.), *Ribonucleases: Structures and Functions*, Academic Press, New York, 1997, pp 305–341.
16. F. M. Richards and H. W. Wyckoff. Bovine pancreatic ribonuclease. In P. D. Boyer (ed.), *The Enzymes,* 3rd ed., vol. 4, Academic Press, New York, 1971, pp. 647–806.
17. M. R. Eftink and R. L. Biltonen. Pancreatic ribonuclease A, the most studied endonuclease. In A. Neuberger, and K. Brocklehurst (eds.), *Hydrolytic Enzymes,* Elsevier Press, New York, pp. 333–376 (1987).
18. R. B. Raffa. *Drug-Receptor Thermodynamics:Introduction and Applications*, John Wiley & Sons, Chichester, 2001.
19. E. Freire, W. W. van Osdol, O. L. Mayorga, and J. M. Sanchez-Ruiz. Calorimetrically determined dynamics of complex unfolding transitions in proteins. *Annu. Rev. Biophys. Biophys. Chem.* **19**:159–188 (1990).
20. M. L. Doyle, D. G. Myszka, and I. M. Chaiken. Molecular interaction analysis in ligand design using mass transport, kinetic and thermodynamic methods. *J. Molec. Recog* **9**:65–74 (1996).
21. R. O'Brien, B. Z. Chowdhry, and J. E. Ladbury. Isothermal titration calorimetry. In S. E. Harding, and B. Z. Chowdhry (eds.), *A Practical Approach to Protein-Ligand Interactions*, Oxford University Press, Oxford, 2001, pp. 263–286.
22. M. J. Todd. and J. Gomez. Enzyme kinetics determined using calorimetry: a general assay for enzyme activity? *Analytic. Biochem* **296**:179–187 (2001).
23. L. Cai, A. Cao, and L. Lai. An isothermal titration calorimetric method to determine the kinetic parameters of enzyme catalytic reaction by employing the product inhibition as probe. *Analytic. Biochem* **299**:19–23 (2001).
24. S. Koerber and A. Fink. The analysis of enzyme progress curves by numerical differentiation, including competitive product inhibition and enzyme reactivation. *Analytic. Biochem* **165**:75–87 (1987).
25. M. Markus, T. Plesser, and M. Kohlmeier. Analysis of progress curves in enzyme kinetics: bias and convergent set in the differential and in the integral method. *J. Biochem. Biophys. Meth* **4**:81–90 (1981).
26. H. Fukuda and K. Takahashi. Enthalpy and heat capacity for the proton dissociation of various buffer components in 0.1M potassium chloride. *Proteins: Struct. Funct. Genetics* **33**:159–166 (1998).
27. T. S. Wiseman, S. Williston, J. F. Brandts, and L.-N. Lin. Rapid measurement of binding constants and heats of binding using a new titration calorimeter. *Analytic. Biochem* **179**:131–137 (1989).
28. R. B. Raffa, S. D. Spencer, and R. J. Schulingkamp. Toward RNase inhibitors: thermodynamics of 2′-CMP/RNase-A binding in multi-ion buffer. *Biochem. Pharmacol.* **63**:1937–1939 (2002).
29. S. D. Spencer, O. Abdul, R. J. Schulingkamp, and R. B. Raffa.

Toward the design of ribonuclease inhbitors: ion effects on the thermodynamics of binding of 2′- CMP to RNase A. *J. Pharmacol. Exper. Ther* **301**:925–929 (2002).
30. J. J. Beintema, C. Schuller, M. Irie, and A. Carsana. Molecular evolution of the ribonuclease superfamily. *Prog. Biophys. Mol. Biol.* **51**:165–192 (1988).
31. J. J. Beintema, W. M. Fitch, and A. Carsana. Molecular evolution of pancreatic-type ribonucleases. *Mol. Biol. Evol.* **3**:262–275 (1986).
32. G. J. Gleich and C. R. Adolphson. The eosinophilic leukocyte: structure and function. *Adv. Immunol.* **39**:177–253 (1986).
33. G. J. Gleich, D. A. Loegering, M. P. Bell, J. L. Checkel, S. J. Ackerman, and D. J. McKean. Biochemical and functional similarities between human eosinophil-derived neurotoxin and eosinophil cationic protein: homology with ribonuclease. *Proc. Natl. Acad. Sci. USA* **83**:3146–3150 (1986).
34. G. J. Gleich, H. Kita, and C. R. Adolphson CR. Eosinophils. In M. M. Frank, K. F. Austen, H. N. Claman, and E. R. Unanue (eds.), *Samter's Immunologic Diseases*, Little Brown, Boston, 1995, pp. 205–245.
35. N. Russo and R. Shapiro. Potent inhibition of mamalian ribonucleases by 3′,5′-pyrophosphate-linked nucleotides. *J. Biol. Chem.* **274**:14902–14908 (1999).
36. G. G. Hammes. *Thermodynamics and Kinetics for the Biological Sciences*, John Wiley & Sons, New York, 2000.
37. R. B. Raffa. Experimental approaches to determine the thermodynamics of protein-ligand interactions. In H-J. Böhm and G. Schneider (eds,), *Protein-Ligand Interactions*, Wiley-VCH, Weinheim, 51–71 (2003).
38. M. Tribout and S. Paredes. and J. Léonis. Investigation of ribonuclease-catalysed kinetics by a micro-calorimetric method. *Biochem. J.* **153**:89–91 (1976).
39. M. R. Eftink and R. L. Biltonin. Energetics of ribonuclease A catalysis. 3. Temperature dependence of the hydrolysis of cytidine cyclic 2′,3′-phosphate. *Biochem.* **22**:5140–5150 (1983).